

See discussions, stats, and author profiles for this publication at: <https://www.researchgate.net/publication/231705048>

# Synthesis and Characterization of Highly Fluorinated Polymer with the Benzoxazine Moiety in the Main Chain

ARTICLE *in* MACROMOLECULES · NOVEMBER 2008

Impact Factor: 5.8 · DOI: 10.1021/ma801253a

---

CITATIONS

59

---

READS

62

4 AUTHORS, INCLUDING:



Hatsuo Ishida

Case Western Reserve University

450 PUBLICATIONS 12,978 CITATIONS

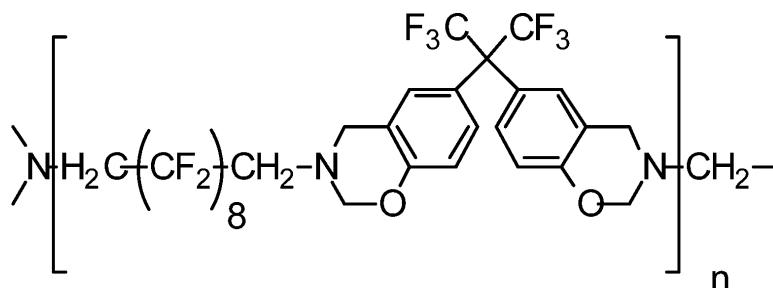
SEE PROFILE

## Synthesis and Characterization of Highly Fluorinated Polymer with the Benzoxazine Moiety in the Main Chain

Pedro Velez-Herrera, Kazuo Doyama, Hiroshi Abe, and Hatsuo Ishida

*Macromolecules*, **2008**, 41 (24), 9704-9714 • DOI: 10.1021/ma801253a • Publication Date (Web): 14 November 2008

Downloaded from <http://pubs.acs.org> on March 14, 2009



Curable Main-chain polybenzoxazine

$$\epsilon = 2.2 \quad \tan \delta = 0.008$$

### More About This Article

Additional resources and features associated with this article are available within the HTML version:

- Supporting Information
- Access to high resolution figures
- Links to articles and content related to this article
- Copyright permission to reproduce figures and/or text from this article

[View the Full Text HTML](#)



**ACS Publications**  
High quality. High impact.

Macromolecules is published by the American Chemical Society, 1155 Sixteenth Street N.W., Washington, DC 20036

# Synthesis and Characterization of Highly Fluorinated Polymer with the Benzoxazine Moiety in the Main Chain

Pedro Velez-Herrera,<sup>\*</sup> Kazuo Doyama,<sup>†</sup> Hiroshi Abe,<sup>†</sup> and Hatsuo Ishida<sup>\*,‡</sup>

NBO Development Center, Sekisui Chemical Co. Ltd., 32 Wadai, Tsukuba, Ibaraki 300-4292, Japan, and Department of Macromolecular Science and Engineering, Case Western Reserve University, Cleveland, Ohio 44106

Received June 4, 2008; Revised Manuscript Received September 30, 2008

**ABSTRACT:** Novel highly fluorinated polymers with the benzoxazine moiety in the main chain have been synthesized by incorporating a highly fluorinated diamine with polyfluorinated bisphenol A. The value of the dielectric constant of the step cured polymer film is 2.20. An analogous hydrogenated version, whose dielectric constant value of 2.8 is also synthesized. The molecular structure of the polymers is characterized by NMR and FT-IR and thermal stability by TGA. The dynamic mechanical properties of the polymer step cured under air and under nitrogen are analyzed.

## 1. Introduction

Polybenzoxazines are a class of thermosetting resins that have been developed over the past decade as an attractive alternative to epoxies, traditional phenolic resins, bismaleimides and even polyimides.<sup>1–6</sup> Benzoxazine resins are synthesized, either in solution or by a melt state reaction, using a combination of a phenolic derivative, formaldehyde, and a primary amine.<sup>7,8</sup> The unique chemistry of benzoxazines is responsible for a number of inherent processing benefits, including low melt viscosity, no volatile release upon cure, and near-zero overall shrinkage. Thermally activated ring-opening polymerization results in a high modulus thermosetting materials with excellent thermal, mechanical and electrical properties.<sup>6</sup>

Thermally activated polymerization of monofunctional benzoxazines typically leads to a linear structure with number average molecular weight on the order of 500–2000 and is characterized by the presence of a Mannich base bridge.<sup>9</sup> The polyfunctionality required to form an infinite network structure upon polymerization can be achieved through monomer synthesis utilizing either a multifunctional phenolic molecules with a monoamine or with a multifunctional amine paired with a monophenol.<sup>10,11</sup> Of these two approaches, the overwhelming majority of polybenzoxazine research published to date has focused on material in which the phenolic compound, typically a bisphenol, provides this multifunctional core. Monofunctional benzoxazine derived from phenol and aniline is cross-linked because the reactivity on the benzene ring creates additional functionality.<sup>10</sup> Recently aliphatic diamines were studied in connection with monofunctional phenols and exhibited outstanding mechanical properties such as flexural modulus, strength, and strain to failure that far surpassed that of typical bisphenol-based polybenzoxazines.<sup>12</sup>

Departing from the majority of monomeric benzoxazine works, reactive oligomers with oxazine ring in the main chain were studied.<sup>13</sup> More detailed work on these class of benzoxazines revealed useful properties, such as low branching and flexible film forming and higher strain to failure, that lead to better mechanical or physical properties.<sup>14</sup> Fluorinated benzoxazine monomers derived from pentafluorophenyl and bisphenol A had been obtained in high yield in an acidic medium. It was

found that the pH value of the reaction medium is the controlling factor in the yield of the compound when a weak amine is used.<sup>1,13</sup> Another fluorinated benzoxazine was synthesized using biphenol-AF and trifluoromethyl aniline. A copolybenzoxazine of this fluorinated benzoxazine with nonfluorinated benzoxazine based on bisphenol A and aniline (BA-a) showed a dielectric constant of 2.36 on 50/50% w/w blend.<sup>15</sup> A porous polybenzoxazine was prepared by treating poly( $\epsilon$ -caprolactone) (pa-PCL) with BA-a type benzoxazine and then hydrolyzed to remove the caprolactone. The porous material showed a dielectric constant value of 1.95 with 25% of pa-PCL. The SEM images showed microphase separation in the matrix. A transition from isolated to interconnected pores was observed when the molecular weight of pa-PCL were increased.<sup>16</sup>

Allen and Ishida synthesized a series of linear aliphatic diamine-based benzoxazines shown in Figure 1. They showed that rate of polymerization is inversely proportional to the aliphatic diamine chain length. The glass transition temperatures decrease with increase in the diamine chain length and the compound with  $n = 6$  was the best option due to its thermal stability and rheological properties.<sup>12</sup> The study of a series of fluoromethylene cyanate esters, Figure 1, shows that the dielectric constant of the material decreases from 2.66 at  $n = 3$  to 2.29 at  $n = 6$  then it increases to 2.31 at  $n = 10$ . The compound with  $n = 6$  was identified as the best compromise for synthesis, properties and processing.<sup>17</sup>

In this paper, a series of highly fluorinated main chain polybenzoxazines having oxazine moieties in the main chain have been synthesized. These reactive main-chain polymers can be further cross-linked via polymerization of the internal oxazine rings and will be hereinafter called main-chain polybenzoxazines. The thermal, mechanical and dielectric

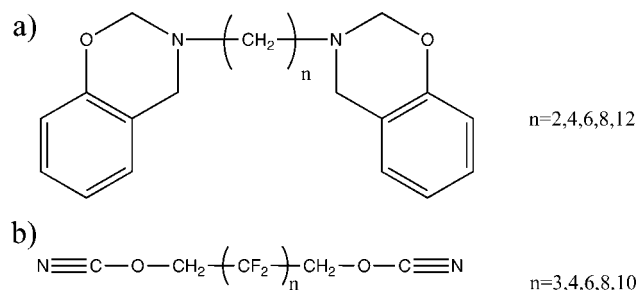


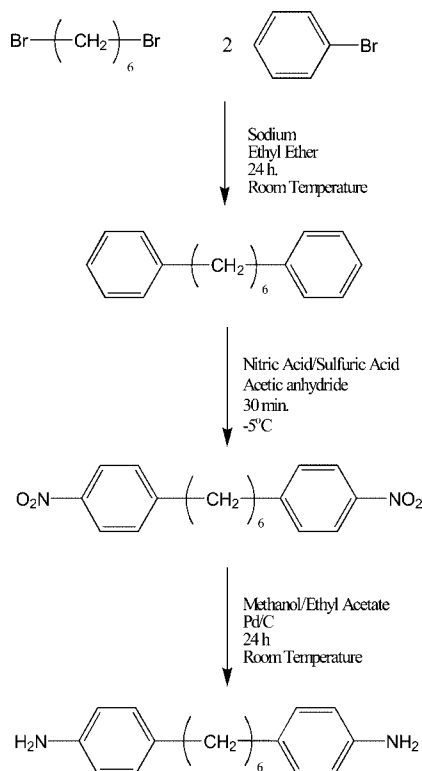
**Figure 1.** (a) Diamine-based benzoxazine monomer and (b) fluoromethylene cyanate ester monomer.

<sup>\*</sup> To whom the correspondence should be addressed.

<sup>†</sup> NBO Development Center, Sekisui Chemical Co. Ltd.

<sup>‡</sup> Department of Macromolecular Science and Engineering, Case Western Reserve University.

## Scheme 1. Synthesis of the Aromatic Hydrogenated Amine



constant properties of the fluorinated benzoxazines are compared against the hydrogenated equivalent main chain polybenzoxazine.

## 2. Experimental Section

**2.1. Materials.** Reagents used for syntheses except for highly fluorinated diamines<sup>18</sup> and 4,4'-diamino-1,6-diphenylhexane are commercially available. Paraformaldehyde (95%), bromobenzene (98%), 1,6-dibromohexane (97%), bisphenol A (97%), and bisphenol AF (98%) were purchased from Aldrich.

**2.2. Equipment.** Thermal transitions were monitored with a differential scanning calorimeter (DSC), Model 2920 Modulated DSC from TA Instruments, and with a DSC, Model 2910 equipped with a Pressure DSC cell also from TA Instruments. Scan rates of 10 K/min over a temperature range of 25 to 300 °C and nitrogen flow rate of 65 mL/min were used in DSC experiments. All samples with masses of 1–3 mg were crimped in hermetically sealed aluminum pans with lids. Transition temperatures were taken from the first heating cycle.

Thermogravimetric analysis (TGA) was performed with a TA Instruments' High Resolution 2950 Thermogravimetric Analyzer that was purged with nitrogen at a flow rate of 90 mL/min as a purge gas. A heating rate of 20 K/min was used.

Dynamic mechanical tests were made under tension mode using a TA Instruments Q800 Dynamic Mechanical Analyzer under a nitrogen atmosphere with a heating rate of 3 K/min using films approximately 3 cm long and 5–8 mm wide, with thickness of about 100–300  $\mu\text{m}$ . Amplitude of 20  $\mu\text{m}$  was applied at a frequency of 1 Hz during each experiment.

The structure of the compound was verified by proton (<sup>1</sup>H), carbon (<sup>13</sup>C) and fluorine (<sup>19</sup>F) nuclear magnetic resonance spectroscopy (NMR) using Varian Inova NMR spectrometer at proton frequency of 600 MHz as well as the corresponding carbon and fluorine frequencies at room temperature using deuterated chloroform as the solvent. Signals were averaged from 256 transients for <sup>1</sup>H NMR and <sup>19</sup>F NMR, and 1024 transients for <sup>13</sup>C NMR to yield spectra with sufficient signal-to-noise ratio.

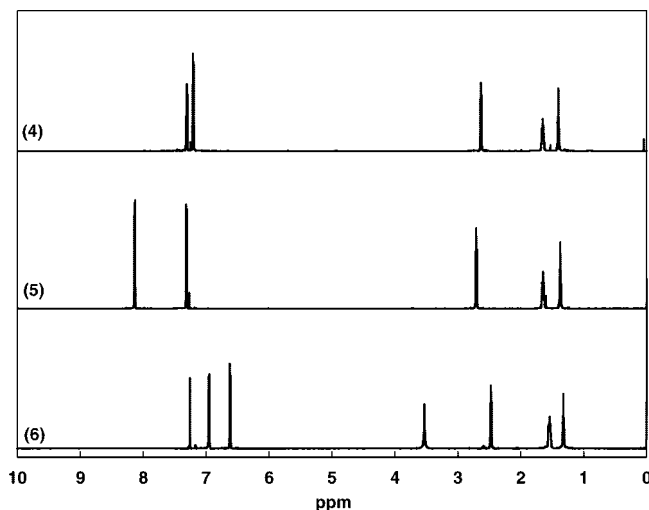


**Figure 2.** <sup>1</sup>H NMR spectra of the hydrogenated aromatic diamine synthesis in CDCl<sub>3</sub> at room temperature.

A relaxation time of 10 s was used for the integrated intensity. <sup>19</sup>F-decoupled NMR spectra were recorded using the waltz16 composite pulse decoupling.

Infrared spectra were recorded using a Bomem Michelson MB100 Fourier transform infrared (FT-IR) spectrometer with deuterated triglycine sulfate (DTGS) detector under dry air purge. Coaddition of 32 scans at a 4 cm<sup>-1</sup> resolution was used.

Size exclusion chromatography (SEC) was carried out using a series of three  $\mu$ Strygel columns with pore size of 10<sup>5</sup>, 10<sup>3</sup>, and 50 nm (Waters) with tetrahydrofuran as eluent. A dual detection system consisting of a refractive index detector (Waters model 410) and ultraviolet (UV) absorption detector (Waters model 440) at a fixed UV frequency of 252 nm was used. A calibration curve was obtained using monodisperse polystyrene reference standards, which were purchased from Toyo Soda, Japan, in THF. The molecular weight of the synthesized polymers was reported referring to this calibration curve.

The dielectric constant and  $\tan \delta$  of the materials were measured by the NBO Development Center at Sekisui Chemical Company using Agilent E4991A RF Impedance/material Analyzer at a frequency of 1 GHz. The measurement cell used was Dielectric Material Test Fixture 16453A. Three points in a thin film with thicknesses ranging from 100 to 500  $\mu\text{m}$  were measured and values averaged. Due to the variation in thickness, the measurement values were reproducible only within 10%.

**2.3. Synthesis.** In this paper ALF8-BF, ALH12-BA, ARF12-BF and ARH12-BA refer to the main chain polybenzoxazines and poly(ALF8-BF), poly(ALH12-BA), poly(ARF12-BF), and poly(ARH12-BA) are the step cured polybenzoxazines derived from the corresponding monomers. Abbreviation shown first is the diamines used and the second abbreviation corresponds to the bisphenols used. Synthetic procedures of those prepolymers having oxazine groups in the main chain other than F8-BF, ARF12-BF, and ARH12-BA followed the published procedures and are thus not described here.<sup>14</sup>

The synthetic route for the aromatic hydrogenated diamine is shown in Scheme 1 and its proton NMR spectrum is presented in Figure 2.

**2.3.1. Synthesis of 1,6-Diphenylpropane (1).** This compound was synthesized using the Wurtz–Fittig reaction.<sup>19</sup> Small pieces of sodium (14 g, 0.6 mol) were covered with 75 mL of anhydrous ethyl ether and a mixture of bromobenzene (40 g, 0.25 mol) and 1,6-dibromohexane (30 g, 0.123 mol) was added. The mixture was placed in an ice bath and stirred for 24 h under nitrogen. The solution was filtered out, washed with water, dried over sodium sulfate and evaporated. The residue was distilled under vacuum. A clear liquid was obtained in 73% yield. (21.5 g, 0.09 mol).

$^1\text{H}$  NMR (chloroform-*d*):  $\delta$  = 7.31 (t, Ar, 4H), 7.21 (s, Ar, 2H), 7.30 (s, Ar, 4H), 2.65 (t,  $-\text{Ar}-\text{CH}_2$ , 4H), 1.65 (m,  $-\text{CH}_2-$ , 4H), 1.40 (m,  $-\text{CH}_2-$ , 4H).

**2.3.2. Synthesis of 4,4'-Dinitro-1,6-diphenylhexane (2).** This compound was prepared according to the general procedure for nitration of an aromatic compound.<sup>20</sup> A nitration medium was prepared by the slow addition of 8 mL of concentrated sulfuric acid and 12 mL of concentrated nitric acid to 40 mL of acetic anhydride, keeping the temperature below  $-5^\circ\text{C}$ . To the medium was added a solution of **1** (30 g, 0.13 mol) in 20 mL of acetic anhydride over a 30 min. After the mixture was stirred at  $-5^\circ\text{C}$  for 45 min., 100 mL of water was added and the mixture was stirred at room temperature for an additional 60 min. The product was washed with water and recrystallized from a mixture of ethanol/hexanes (90/10). Yellow flake-like crystals were obtained in 54% yield (23 g, 0.07 mol).

$^1\text{H}$  NMR (chloroform-*d*):  $\delta$  = 8.13 (d, Ar, 4H), 7.31 (d, Ar, 4H), 2.70 (t,  $-\text{Ar}-\text{CH}_2$ , 4H), 1.65 (m,  $-\text{CH}_2-$ , 4H), 1.40 (m,  $-\text{CH}_2-$ , 4H).

**2.3.3. Synthesis of 4,4'-Diamino-1,6-diphenylhexane (3).** **2** (5 g, 15 mmol) was catalytically hydrogenated with 10% Pd-C (0.2 g) in 100 mL of methanol/ethyl acetate (50/50) for 24 h at room temperature. The solution was filtered with celite, and evaporated under vacuum. The product was obtained quantitatively and used without any purification. (4 g, 14.8 mmol).

$^1\text{H}$  NMR (chloroform-*d*):  $\delta$  = 6.95 (d, Ar, 4H), 6.61 (d, Ar, 4H), 3.53 (s,  $-\text{NH}_2$ , 4H), 2.50 (t,  $-\text{Ar}-\text{CH}_2$ , 4H), 1.54 (m,  $-\text{CH}_2-$ , 4H), 1.40 (m,  $-\text{CH}_2-$ , 4H).

The synthetic routes for the main chain polybenzoxazines are shown in Schemes 2 and 3.

**2.3.4. Synthesis of F8-BF.** The synthesis of highly fluorinated diamines is more complex and is reported elsewhere.<sup>18</sup>

Paraformaldehyde (2.3 g, 77 mmol) and bisphenol AF (6.5 g, 19.2 mmol) were added to a solution of 2,2,3,3,4,4,5,5-octafluorohexane-1,6-diamine **4** (5 g, 19.2 mmol) in chloroform (50 mL) and catalytic amount of triethylamine. The mixture was stirred for 8 h at reflux temperature. The solvent was evaporated under vacuum. The solids were washed with hexanes, filtered out and dried under vacuum. A white powder was obtained 85% yield (10.8 g, 16.3 mmol). Anal. Calcd: C, 45.40; H, 3.20; N, 6.35. Found: C, 45.90; H, 4.51; N, 5.84.

$^1\text{H}$  NMR (chloroform-*d*):  $\delta$  = 7.98 (m, Ar, 2H), 7.12 (m, Ar, 2H), 6.80 (m, Ar, 2H), 4.86 (s,  $\text{O}-\text{CH}_2-\text{N}<$ , 4H), 4.07 (s,  $>\text{N}-\text{CH}_2-\text{Ar}$ , 4H), 3.42 (s,  $>\text{N}-\text{CH}_2-\text{CF}_2$ , 4H).

$^{19}\text{F}$  NMR (chloroform-*d*):  $\delta$  =  $-64$  (s,  $-\text{CF}_3$ , 6F),  $-118$  (s,  $-\text{N}-\text{CH}_2-\text{CF}_2-$ , 4F),  $-123$  (s,  $>\text{N}-\text{CH}_2-\text{CF}_2-\text{CF}_2-$ , 4F).

**2.3.5. Synthesis of ARF12-BF.** A 20% w/w solution of paraformaldehyde (1.24 g, 41.2 mmol), bisphenol AF (3.5 g, 10.3 mmol), and 4,4'-(perfluorohexane-1,6-diyl) dibenzeneamine, **5** (5 g, 10.3 mmol) in chloroform was prepared. The mixture was stirred for 72 h at reflux temperature. The solvent was evaporated under vacuum. A yellow powder in 89% yield was obtained (8.1 gr, 9.17 mmol).

Anal. Calcd: C, 50.18; H, 2.85; N, 4.74. Found: C, 49.97; H, 3.20; N, 3.59.

$^1\text{H}$  NMR (chloroform-*d*):  $\delta$  = 7.47 (m, Ar, 4H), 7.12 (m, Ar, 4H), 7.05 (m, Ar, 2H), 6.80 (m, Ar, 4H), 5.40 (s,  $\text{O}-\text{CH}_2-\text{N}<$ , 4H), 4.65 (s,  $>\text{N}-\text{CH}_2-\text{Ar}$ , 4H).

$^{19}\text{F}$  NMR (chloroform-*d*)  $\delta$  =  $-64$  (s,  $\text{C}-\text{CF}_3$ , 6F),  $-109$  (s,  $\text{Ar}-\text{CF}_2-\text{CF}_2$ , 4F),  $-121$  (s,  $\text{Ar}-\text{CF}_2-\text{CF}_2-$ , 4F),  $-122$  (s,  $\text{Ar}-(\text{CF}_2)_2-\text{CF}_2-$ , 4F).

**2.3.6. Synthesis of ARH12-BA.** A 10% w/w solution of paraformaldehyde (1.24 g, 41.2 mmol), bisphenol A (2.35 g, 10.3 mmol), and **3** (2.75 g, 10.3 mmol) in chloroform was prepared. The mixture was stirred for 8 h at reflux temperature. The solvent was evaporated under vacuum. A powder in 91% yield was obtained (5.27 g, 9.4 mmol).

Anal. Calcd: C, 79.11; H, 7.72; N, 7.48. Found: C, 79.46; H, 7.46; N, 7.93.

$^1\text{H}$  NMR (chloroform-*d*):  $\delta$  = 7.04 (d, Ar, 4H), 7.01 (d, Ar, 4H), 6.92 (d, Ar, 2H), 6.82 (s, Ar, 2H), 6.68 (d, Ar, 2H), 5.29 (s,

$\text{O}-\text{CH}_2-\text{N}<$ , 4H), 4.53 (s,  $>\text{N}-\text{CH}_2-\text{Ar}$ , 4H), 2.50 (t,  $-\text{Ar}-\text{CH}_2$ , 4H), 1.59 (m,  $-\text{CH}_3$ , 6H), 1.54 (m,  $-\text{CH}_2-$ , 4H), 1.40 (m,  $-\text{CH}_2-$ , 4H).

**2.3.7. Synthesis of 3,3'-(4,4'-(Perfluorohexane-1,6-diyl)bis(4,1-phenylene))bis(6-fluoro-3,4-dihydro-2H-benzoxazine) (ARF12M) (Scheme 4).** Synthesis of this compound has been reported elsewhere.<sup>18</sup>

**2.4. Sample Preparation.** Polymerized samples of reactive main-chain polybenzoxazines were prepared for dynamic mechanical analysis, thermogravimetric analysis, density measurement, and water absorption in the following manner: A 20–25% by weight solution of each sample in dimethylformamide (DMF) was placed over a Teflon sheet. The solvent was evaporated at room temperature for 24 h. The samples were dried at room temperature overnight in vacuum to minimize any trace of solvent. The reactive main-chain polybenzoxazines were then step cured in a convection oven or in a closed oven under a nitrogen atmosphere for 60 min at 100, 125, 150, 175, and 200  $^\circ\text{C}$ . Upon completion of the curing, the samples were allowed to freely cool to room temperature. Individual test samples were cut to appropriate dimensions and then polished until visually smooth.

**2.5. Water Absorption.** The cured samples were conditioned under vacuum at 90  $^\circ\text{C}$  for 24 h before placing in the environment of air (100% RH) or water for one day and one week. All these experiments were conducted at room temperature. Then, the percentages of water absorption of the cured samples were calculated. While the length of the experiment was not very long, the equilibrium water up-take was likely achieved due to the thin samples used. The sample dimension described in ASTM could not be employed due to the limited amount of the polymers available. The dimension of the samples used was 50 mm  $\times$  20 mm  $\times$  0.35 mm. The thickness value is the average thickness.

### 3. Results

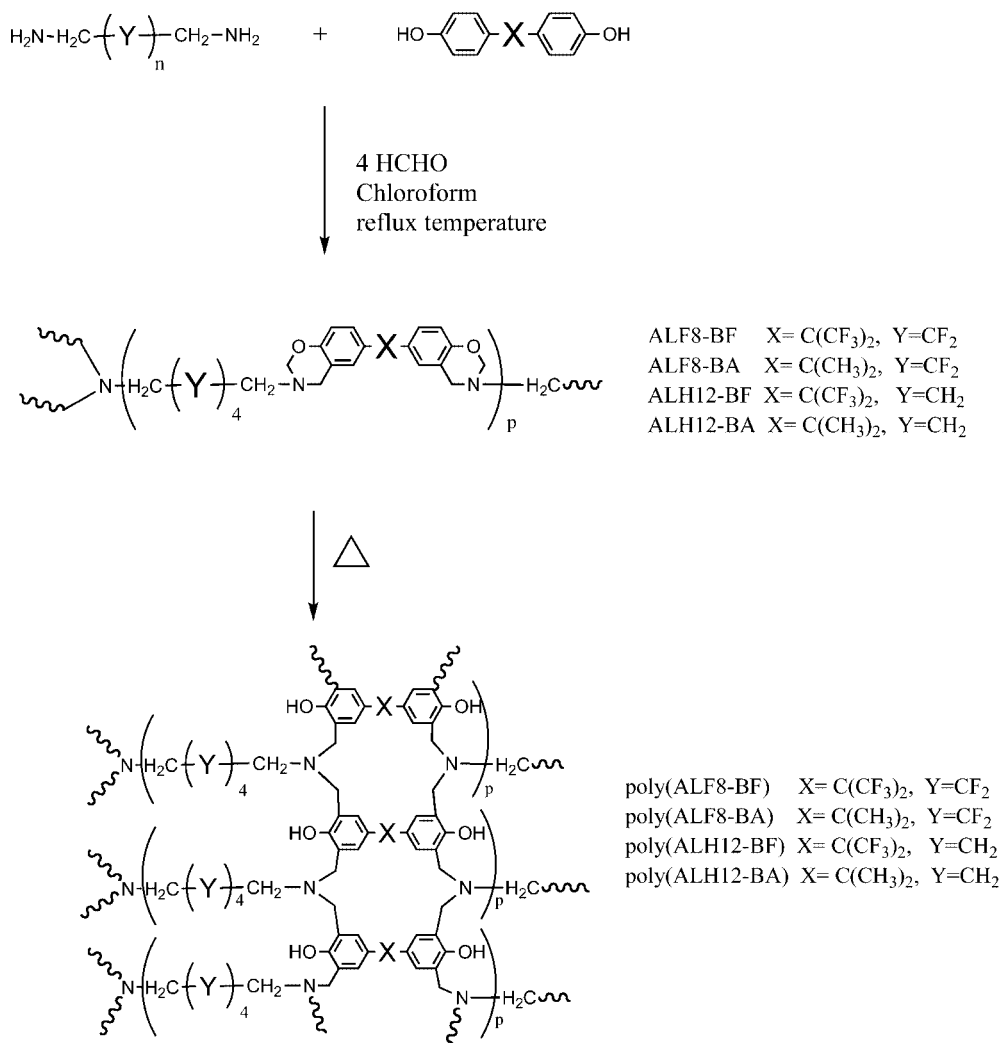
The synthesis and structure of polymers are shown in Schemes 2 and 3. The structure of the cured main-chain polybenzoxazines will be complicated and the written structures are not meant to be literally taken. All reactive main-chain polybenzoxazines were obtained in satisfactory yields. The observed  $^1\text{H}$  NMR,  $^{13}\text{C}$  NMR,  $^{19}\text{F}$  NMR and FTIR signals agree well with the expected chemical structure.

**3.1. Analysis of the Main Chain Polymer. 3.1.1. Nuclear Magnetic Resonance Spectroscopy.** Both the NMR and FTIR spectroscopic analyses of the main chain polymer confirmed the structure of the fluorinated and hydrogenated diamine-based benzoxazine polymers. The proton NMR spectra for the aliphatic diamine-based benzoxazines are shown in Figure 3. Each spectrum shows two resonances centered at 4.0 and 4.8 ppm, which are consistent with the formation of a benzoxazine ring. The very weak resonance around 4.6 ppm has been assigned to the methylol group. Mannich bridge protons of open oxazine rings are typically located at approximately 3.7 ppm. Aromatic diamine-based benzoxazines have the oxazine resonances at 4.6 and 5.3 ppm, and the triazine group is around 5.0 ppm, as seen in Figure 4. The influence of the fluorine in the chemical shift can be seen on the position of the oxazine related resonances. For the aliphatic amine, the separation between resonances decreases from 0.89 to 0.79 ppm when the hydrogen is partially substituted by fluorine. In the case of the aromatic amine the chemical shift increases by 0.1 ppm when going from hydrogenated to fluorinated amine, but the separation between both stays constant at 0.75 ppm. The  $^{13}\text{C}$  NMR spectra of the main chain polymers are presented in Figure 5. The exact positions for the proton NMR chemical shift of the oxazine related resonances are listed in Table 1.

**3.1.2. Infrared Spectroscopy.** Figure 6 shows the FT-IR spectra of the reactive main-chain polybenzoxazines at room temperature. The absence of a vibrational peak for free or



Scheme 2. Synthesis of the Aliphatic Amine-Based Polymer with the Benzoxazine Moiety on the Main Chain



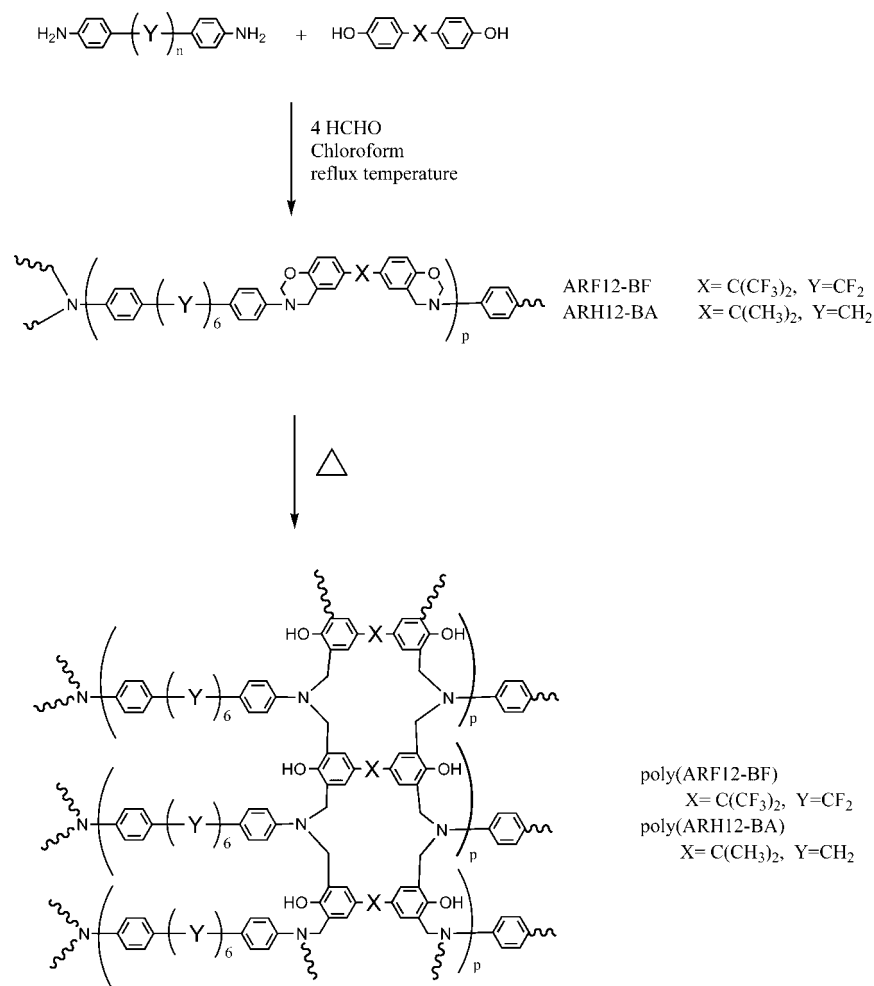
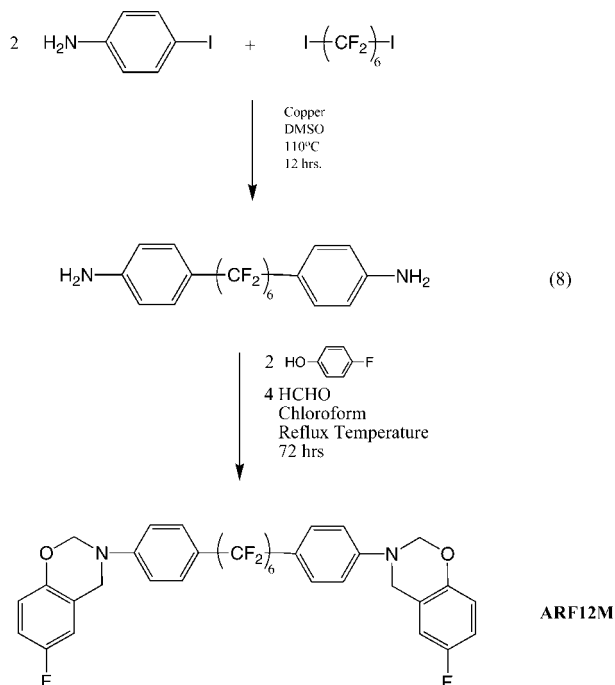
relatively free hydroxyl groups, which have been shown to absorb above  $3600\text{ cm}^{-1}$  in model benzoxazine compounds, suggests that all the phenolic hydroxyl groups are involved in some form of intra- or intermolecular hydrogen bonding.<sup>12,24,25</sup> The difference in the spectra across this region seems to indicate that there are variation in the form or type of hydrogen bonding that occurs in each polymer network. **ALF8-BF** shows the strongest  $-\text{OH}\cdots\text{N}$  intramolecular hydrogen bonding generated by Mannich bridge as indicated by the band located at approximately  $3180\text{ cm}^{-1}$ .<sup>24,25</sup> Aromatic-based diamine compounds, **ARF12-BF** and **ARH12-BA**, show hydroxyl-bonded hydroxyl peak around  $3310\text{ cm}^{-1}$  and thus appears to have  $-\text{OH}\cdots\text{O}$  intermolecular hydrogen bonding. A similar band is seen in bisphenol/aromatic amine-based polybenzoxazines.<sup>12</sup>

The infrared spectra of the main chain polybenzoxazines over the fingerprint region before polymerization show several infrared bands common to both spectra. The presence of the aromatic ether of the benzoxazine ring is confirmed by the absorbance peak around  $1240\text{--}1230$  and  $1040\text{--}1030\text{ cm}^{-1}$ , due to the C—O—C antisymmetric and symmetric stretching modes, respectively.<sup>26</sup> The absorbance between  $955$  and  $945\text{ cm}^{-1}$  are characteristic modes of benzene with an attached oxazine ring. The band at  $1501\text{ cm}^{-1}$  is characteristic of asymmetric trisubstituted benzene. The bands between  $1200$  and  $1100$  are assigned to the CF<sub>2</sub> stretching. The CF<sub>3</sub> group shows a strong absorbance at  $1172\text{ cm}^{-1}$ .<sup>27</sup> The absorbance at  $1160$ ,  $1204$  and  $1336$  are related to the C—N—C of the unreacted 1,3,5-triazine.<sup>28</sup> All the

compounds show a strong band at  $1615\text{ cm}^{-1}$  which is related to the  $-\text{C}=\text{C}-$  quadrant stretching of the para-substituted benzene ring. Table 1 shows the characteristic absorbance of the benzene ring attached to an oxazine ring for the polymers.

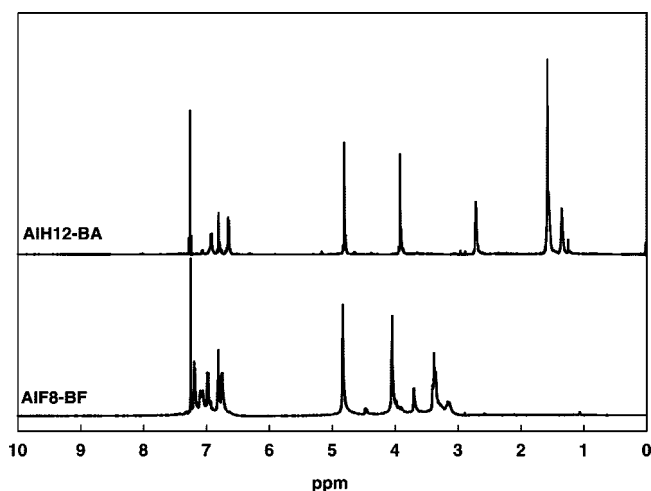
**3.1.3. Size Exclusion Chromatography of The Main Chain Polybenzoxazine.** The results from the size exclusion chromatography are summarized in Table 2. The SEC chromatograms, Figure 7, suggest polymers with a degree of polymerization (DP) between 10 and 18 and polydispersity index (PDI) between 2.5 and 2.8 for all the compounds except for **ALH12-BA** that has a PDI of 3.2. It has been established that molecular weight and polydispersity of main chain benzoxazines depend on the reaction time and the broadening of distribution is caused by side reactions during synthesis of the linear polymer.<sup>13,29</sup> The proposed branches could be created by<sup>13,28</sup> (1) the reaction of the aminomethylol species with the oxazine ring in the polymer main chain, (2) the partially open triaza ring, and (3) benzoxazine ring opening by free phenolic structures, as seen in Figure 8. A Mannich bridge is formed in the first two cases. The presence of Mannich bridge and 1,3,5-triazia compounds was confirmed by proton NMR and FTIR as described before. The limited molecular weight of the polymer was explained by the incomplete conversion of the reaction.<sup>13</sup>

**3.1.4. Differential Scanning Calorimetry of The Main Chain Polybenzoxazine.** The DSC thermograms of the main chain polybenzoxazines, presented in Figure 9, did not show melting transition for any of the samples. Aliphatic diamine-based

**Scheme 3. Synthesis of the Aromatic Amine-Based Polymer with the Benzoxazine Moiety on the Main Chain****Scheme 4. Synthesis of the Fluorinated Aromatic Amine-Based Benzoxazine Monomer Proposed in This Work**

compounds show two distinctive exothermic peaks: the first one at 180 °C has been previously assigned to the cross-linking

reaction of benzoxazine due to the catalytic effect of the methylol end groups and the one at higher temperature, around 250 °C, is related to the conventional benzoxazine polymerization.<sup>13</sup> The presence of methylol group in the aliphatic diamine-based polybenzoxazines was confirmed by NMR and infrared spectroscopy. The DSC thermogram for the aromatic diamine-based polybenzoxazines show the normal exotherm polymerization around 230 °C for both polymers. The absence of the low temperature peak is due to low concentration of methylol

**Figure 3.** <sup>1</sup>H NMR of the aliphatic diamine-based main chain polybenzoxazines in CDCl<sub>3</sub> at room temperature.

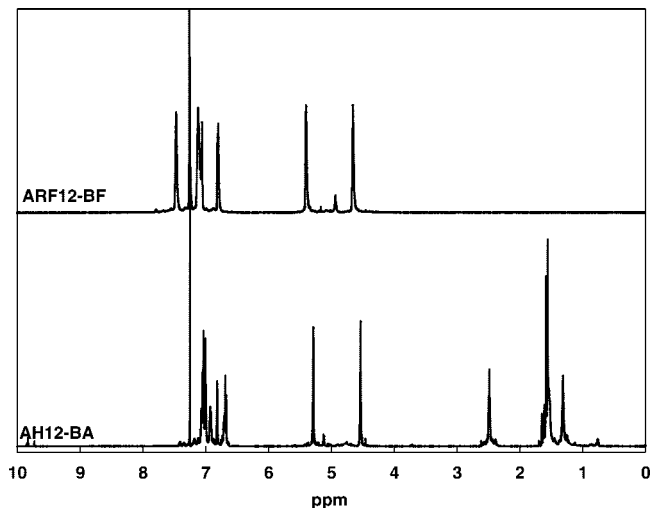


Figure 4.  $^1\text{H}$  NMR of the aromatic diamine-based main chain polybenzoxazines in  $\text{CDCl}_3$  at room temperature.

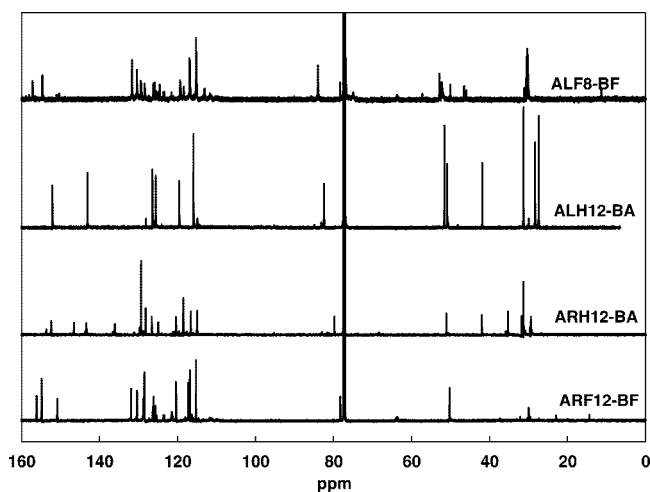


Figure 5.  $^{13}\text{C}$  NMR spectra of the diamine-based polybenzoxazines in  $\text{CDCl}_3$  at room temperature.

Table 1. Summary of the Results of FTIR and NMR Spectroscopy for the Main Chain Polybenzoxazines

compound	NMR (ppm)				FTIR (cm <sup>-1</sup> )
	Ar-CH <sub>2</sub> -N		O-CH <sub>2</sub> -N		
	<sup>1</sup> H	<sup>13</sup> C	<sup>1</sup> H	<sup>13</sup> C	
ALF8-BF	4.06	52.84	4.85	83.98	948
ALH12-BA <sup>a</sup>	3.92	50.94	4.81	82.54	931
ARF12-BF	4.65	50.22	5.40	78.30	947
ARH12-BA	4.53	51.07	5.29	79.76	946

<sup>a</sup> Taken from Chernykh, A.; Liu J.; Ishida, H. *Polymer* **2006**, 47, 7664.

group as indicated by proton NMR and by the fact that aromatic amines tend to form 1,3,5-triaza compounds from the methylol. Unlike methylol group, triazas do not decrease the polymerization temperature of benzoxazines.<sup>7,28</sup> The  $^1\text{H}$  NMR spectra of the aromatic diamine-based polymers show the presence of 1,3,5-triaza compounds.

**3.2. Analysis of the Step Cured Main-Chain Polybenzoxazines.** **3.2.1. Step Cured Polymerization.** The FTIR spectra (see the supplement) of the curing process for the main-chain polymers show that no change was observed after 60 min. at 100  $^\circ\text{C}$ , but after an additional hour at 125  $^\circ\text{C}$ , the absorbance

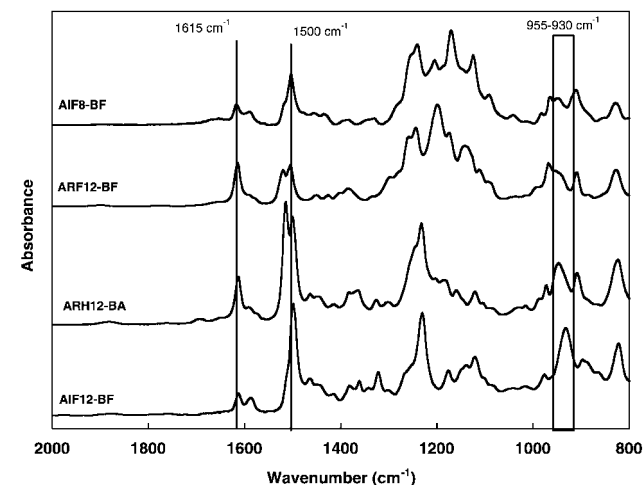
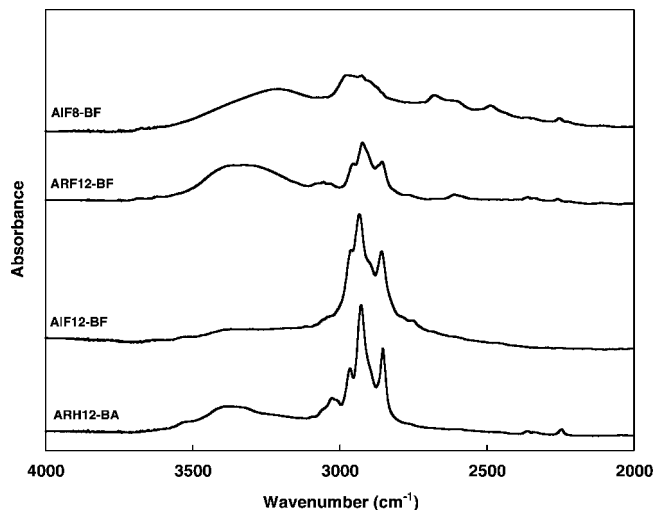


Figure 6. FTIR of the hydroxyl area (top) and fingerprint area (bottom) of the main chain polymers.

Table 2. Summary of the Results of Size Exclusion Chromatography for the Main Chain Polybenzoxazines<sup>a</sup>

compound	$M_w$ of the repeat unit	$M_n$	PDI	$X_n$
ALF8-BF	658	6645	2.74	10
ARF12-BF	882	13332	2.70	15
ALH12-BA	403	7329	3.27	18
ARH12-BA	558	6476	2.56	11

<sup>a</sup> The molecular weights are reported with respect to monodisperse polystyrene reference standards.

at 950–930 and 1520  $\text{cm}^{-1}$  started to decrease in intensity indicating the opening of the oxazine ring and the polymerization of the main chain polybenzoxazine, respectively. The fact that the changes occur at relatively low temperature is because the end groups, phenols and aminomethylol, act as catalyst.<sup>13,30</sup> The fingerprint region of the sample at 150  $^\circ\text{C}$  also shows the carbonyl band at 1680  $\text{cm}^{-1}$  and a radial benzene mode at 1252  $\text{cm}^{-1}$ , suggesting degradation of the polybenzoxazines.<sup>21</sup> The sample was fully polymerized at 200  $^\circ\text{C}$  as indicated by the disappearance of the absorbance at 950–930  $\text{cm}^{-1}$  and the corresponding band at 1520  $\text{cm}^{-1}$ .

**3.2.2. Infrared Spectroscopy.** During the polymerization of the benzoxazines, a phenolic group hydroxyl group is theoretically produced for every oxazine ring that is opened. Previous research has shown that hydrogen bonding of this hydroxyl groups plays an important role in the network structure of polybenzoxazines and may contribute to many of their physical and mechanical properties.<sup>6,25</sup> The hydroxyl region for each of



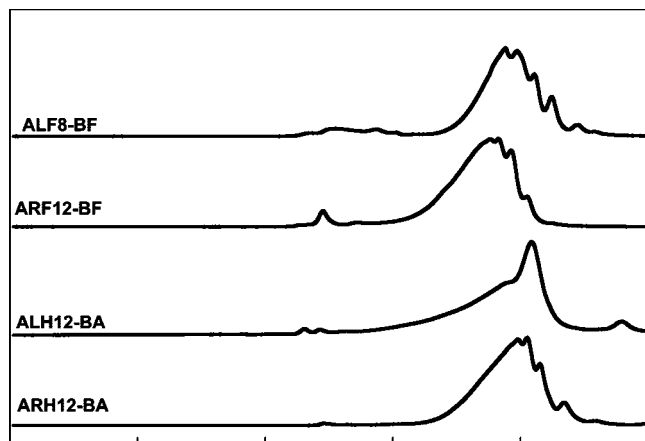


**Figure 7.** Size exclusion chromatogram of the main chain polybenzoxazines.

the cured hydrogenated polymer is given in the supplement. Each polymer spectrum shows the vibrational peak for free hydroxyl group that absorb above  $3600\text{ cm}^{-1}$  in model benzoxazine dimers.<sup>25</sup> This is more evident on the cured hydrogenated polymers than in the step cured fluorinated polymers, and suggests that not all the phenolic hydroxyl groups are involved in hydrogen bonding. The spectral differences among the cured polymer across this region would also seem to indicate that there is some variation in the form or type of hydrogen bonding that occurs in each polymer network. The lowest frequency hydroxyl bands in the fluorinated materials is located at approximately  $3330\text{ cm}^{-1}$  suggesting  $\text{-OH}\cdots\text{O}$  intermolecular hydrogen bonding. A similar absorbance band is seen in bisphenol/aromatic amine-based, methyl substituted phenol and diamine-based polybenzoxazines.<sup>12,25,31</sup> For the hydrogenated polymers, the lowest frequency is located at  $3180\text{ cm}^{-1}$ . This is consistent with the  $\text{-OH}\cdots\text{N}$  intramolecular hydrogen bonding of the Mannich bridge. Hydrogenated cured polymers also show a weak intramolecular absorption band at  $3520\text{ cm}^{-1}$ , which can be assigned to  $\text{-OH}\cdots\pi$  hydrogen bonding.<sup>24</sup> This band was absent in the fluorinated polymers.

The FTIR spectra of the fingerprint area of the cured aliphatic polymer are also given in the supplement. For each polymer, the absorbance bands indicating the oxazine ring at  $920$  and  $950\text{ cm}^{-1}$  have completely disappeared. The bands in the  $1500\text{--}1400\text{ cm}^{-1}$  region confirmed the formation of 1,2,3,5-tetrasubstituted benzene groups. A substituted benzoquinone formation is also seen near  $1680\text{ cm}^{-1}$ .

**3.2.3. Thermogravimetric Analysis.** The results of the thermogravimetric analysis of the main chain polybenzoxazines are summarized in Table 3, while the weight loss and derivative weight loss curves are presented in Figures 10 and 11. The group next to the amine plays an important role on the onset degradation temperature. The temperature of 1% weight loss is above  $300\text{ }^{\circ}\text{C}$  for the aromatic-based diamine, and close to  $280\text{ }^{\circ}\text{C}$  for the aliphatic-based compounds. From the derivative weight loss, it is apparent that fluorine plays an important role in the degradation of step cured main chain polybenzoxazines. Figure 10 shows a faster weight loss for the hydrogenated amine. This phenomena is observed between  $350$  and  $500\text{ }^{\circ}\text{C}$ , because  $\text{C-H}$ ,  $\text{C-C}$ , and  $\text{C-N}$  bonds of aliphatic polymers generally become unstable at temperatures above  $400\text{ }^{\circ}\text{C}$  even in nitrogen environment.<sup>15</sup> The same phenomenon was observed when BA-a and bisphenol AF-aniline based benzoxazine (BF-a) are compared.<sup>1</sup> Organic materials composed of nonaliphatic  $\text{C-H}$ ,  $\text{C-C}$ , and  $\text{C-N}$  such as aromatic structures are able to resist elevated temperatures.<sup>1,30</sup>

**3.2.4. Dynamic Mechanical Analysis.** The dynamic mechanical properties of the step cured main chain polybenzoxazines

were measured from room temperature to beyond the glass transition temperature ( $T_g$ ) of each material. The storage modulus,  $E'$ , for this series of main chain polybenzoxazine is presented in Figure 12. The storage modulus at room temperature is around  $2.0\text{ GPa}$  for all the compounds. This value is between  $2.2\text{ GPa}$  observed for the most commonly studied polybenzoxazine, BA-a<sup>6</sup> and the value of  $1.6\text{ GPa}$  observed for the phenol-hexanediamine based benzoxazine (P-ad6).<sup>12</sup> BA-a has also a rigid aromatic bisphenol compound for its backbone.<sup>6</sup>

In the transition zone, the storage modulus of the polybenzoxazines depends on the type of the amine used. It becomes less stiff as the methylene group is used instead of a phenyl group. The difference between aromatic and aliphatic based-diamines is obvious as the modulus for the aromatic compound is always higher than that of the corresponding aliphatic counterpart. The infrared spectrum of the aromatic based diamine shows a different degree of hydrogen bonding when compared to the aliphatic based diamine. Since hydrogen bonding has been shown to play an important role in the properties of benzoxazines, it is likely that the elastic modulus is influenced by the difference in hydrogen bonding.<sup>6,25</sup>

The glass transition temperature ( $T_g$ ) is an important property of the dielectric constant film. The modulus significantly decreases above  $T_g$  and typically results in a shift in the dielectric properties. Therefore, a polymer with  $T_g$  greater or equal to the highest processing temperature is desirable.<sup>15</sup> The loss modulus spectrum or viscous component,  $E''$ , for each step cured main chain polybenzoxazine is shown in Figure 13. The glass transition temperature of each material can be determined for the maximum peak of the loss modulus. The  $T_g$  observed is close to  $160\text{ }^{\circ}\text{C}$  for the aromatic diamine-based polymers, while  $180\text{ }^{\circ}\text{C}$  for **poly(ALF8-BF)**. These polybenzoxazines have  $T_g$  equivalent to BA-a and P-ad6, which have transitions near  $170\text{ }^{\circ}\text{C}$ . A value of  $230\text{ }^{\circ}\text{C}$  was found for **poly(ALH12-BA)**.

The cross-link density of a thermosetting resin may be estimated from the rubbery plateau modulus using an equation from the statistical theory of rubber elasticity theory:<sup>32</sup>  $G_e = \phi RT = \phi(\rho/M_c)RT$ , where  $G_e$  is the equilibrium share modulus in the rubbery region,  $\phi$  is a front factor, which is unity for ideal rubbers,  $R$  is the gas constant, and  $T$  is the absolute temperature. The cross-link density or concentration of network chain,  $\nu$ , is the number of moles of network chains per unit volume of the cured polymers. If the density of the polymer,  $\rho$ , is known, then the molecular weight between cross-links,  $M_c$ , may also be calculated. However, this equation is strictly valid only for lightly cross-linked materials and, therefore, can only be used to qualitatively compare the level of cross-linking among the various polybenzoxazines and for comparison with other thermosets, whose reported values were calculated in a similar manner.

Analysis of cross-link densities for **poly(ALH12-BA)** is complicated by thermal degradation above the glass transition temperature. The degradation appears to prevent the formation of the rubbery plateau for this compound, and, thus, the value of the plateau modulus in this region is unobtainable. Due to the lower glass transition temperature of other three polymers, the rubbery plateaus are stable with moduli that can be roughly determined between  $17$  and  $20\text{ MPa}$  at a temperature of  $T_g + 50\text{ }^{\circ}\text{C}$ . These values for the modulus in the rubbery plateau were used to estimate the cross-link density and molecular weight between cross-links for the latter three polybenzoxazines and are summarized in Table 4.

The molecular weight between cross-links ( $M_c$ ) for these materials is above  $350$  for the fluorinated compounds and around  $200$  for the hydrogenated diamine. The  $M_c$  of the diamine-based polybenzoxazine can be normalized to the molecular weight of the repeat unit in order to roughly determine the number of

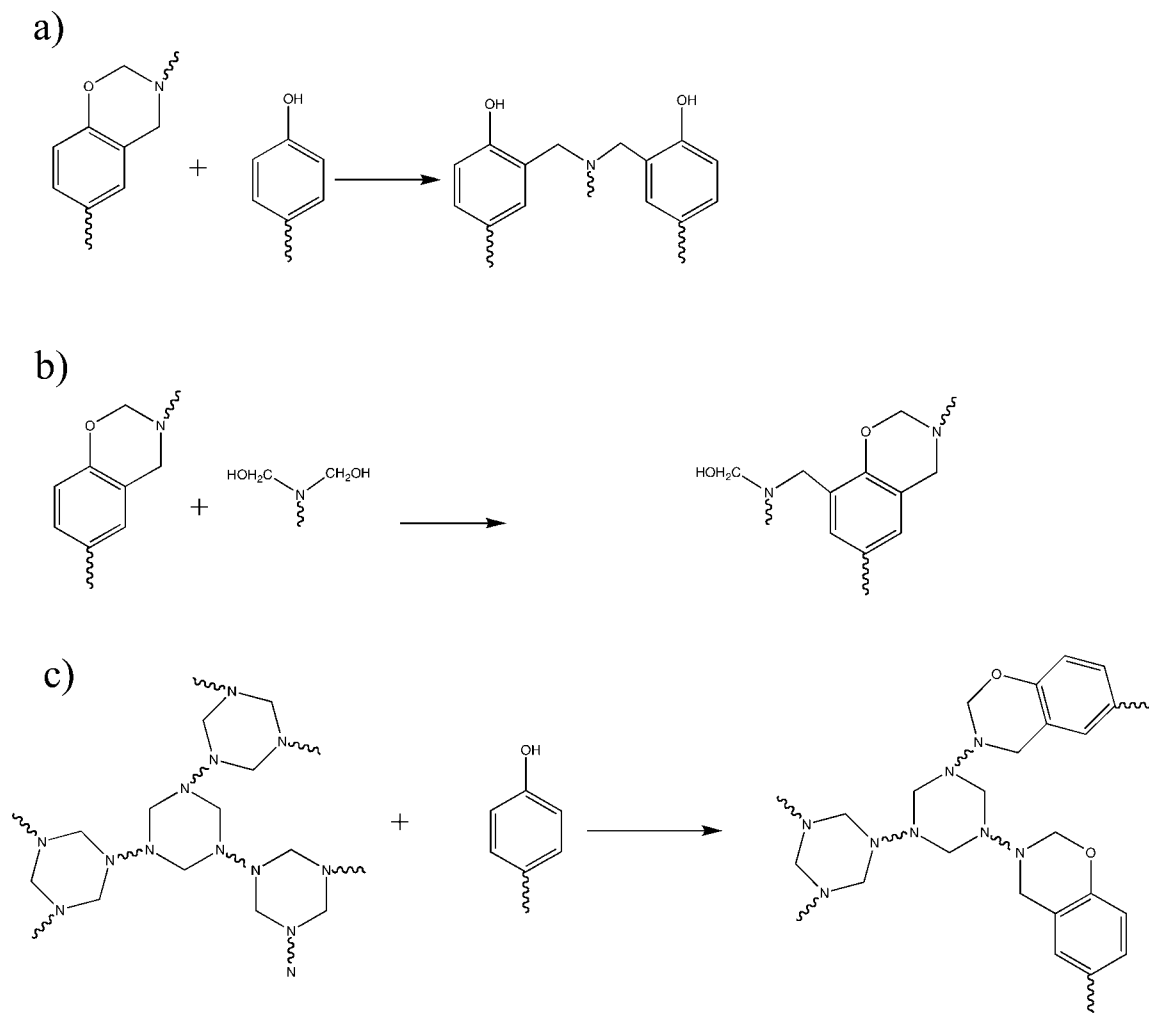


Figure 8. Suggested mechanism of branching formation during the main chain benzoxazine synthesis. (a–c) 1,3,5-Triaza compounds.

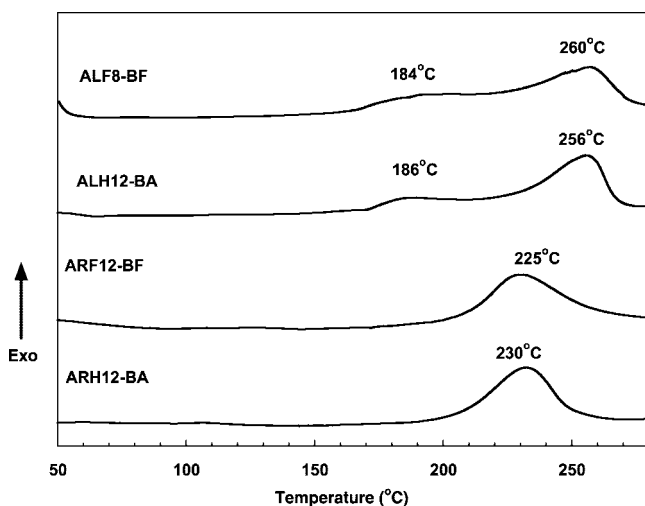


Figure 9. Nonisothermal DSC thermogram of main chain polybenzoxazines under nitrogen environment.

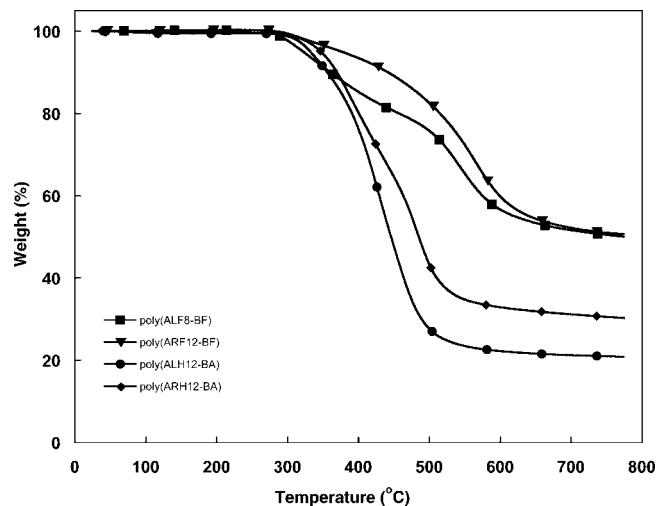
cross-links per chemical repeat unit. A value of 2.3 was obtained for the aromatic-based diamine polymers. This value is very close to 2.2 cross-links per units obtained for P-ad6 and implies that during polymerization, the open oxazine rings must be attached not only to the free ortho-position on the phenol, but also, to a limited degree, at an additional site. Studies of BA-a have shown that, in fact, the arylamine rings can undergo an aminomethylation reaction during the polymerization.<sup>4</sup> The

Table 3. Summary of the Results of the Thermogravimetric Analysis of the Polybenzoxazine Monomers Step Cured

	poly (ALF8-BF)	poly (ARF12-BF)	poly (ARH12-BA)	poly (ALH12-BA)
fluorine content (%)	40.21	38.62	0.0	0.0
temperature 1% (°C)	284	308	301	286
temperature 5% (°C)	322	377	347	332
temperature 10% (°C)	360	441	370	355
char yield (%)	50	50	30	20

constant numbers of cross-links per repeat unit would also seem to indicate that these two polybenzoxazines have a similar polymerization mechanism and network structure, varying only in the nature of the aliphatic chain, but not in the position of the cross-links.

The cross-links per unit calculated for **poly(ALF8-BF)** is 1.8. This value is lower than the cross-link per unit obtained for the aromatic based-diamine polybenzoxazine. The reason is because there is not an arylamine ring that provide the additional site to further increase the cross-linking of the material. The only possible site for the aminomethylation reaction is on the bisphenol core. The value of 1.8 is in between 2.2 for P-ad6 and that of 1.1 obtained for the *p*-cresol–hexanediamine based benzoxazine (cP-ad6); both polymers contain an aliphatic diamine and the only difference is in the phenolic moiety.



**Figure 10.** Percent weight loss for polybenzoxazine step cured during thermogravimetric analysis in a nitrogen environment.

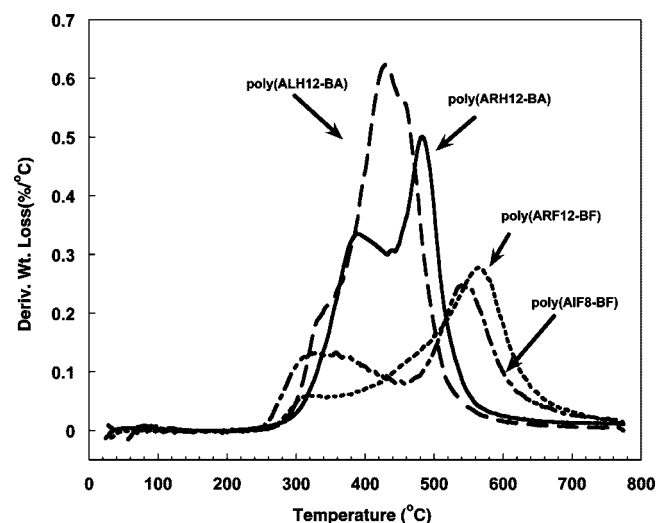


**Figure 11.** Derivative weight loss for polybenzoxazine step cured during thermogravimetric analysis in a nitrogen environment.

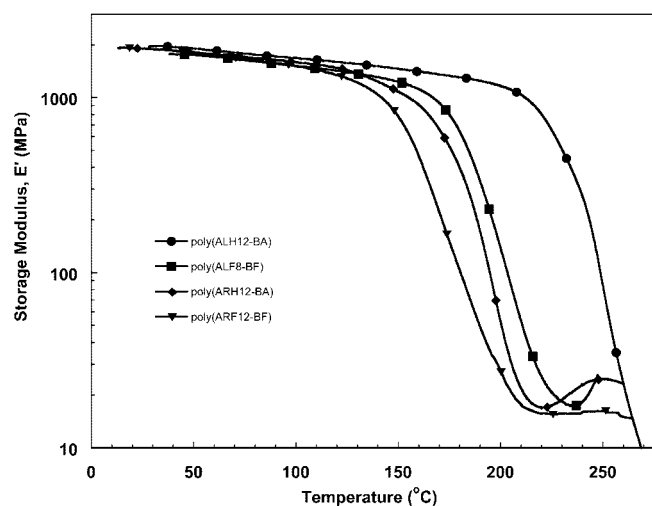


**Figure 12.** Storage moduli for the diamine-based series of polybenzoxazines step cured under air.

The  $T_g$  difference between the aliphatic and aromatic systems seems to be counterintuitive, considering the higher cross-link density of the aromatic system. It is probably due to the following reasons. Glass transition temperature is highly

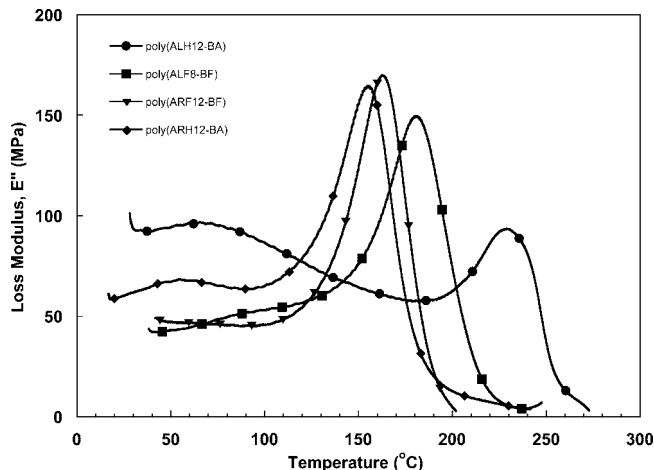


**Figure 13.** Loss moduli for the diamine-based series of polybenzoxazines step cured under nitrogen.

**Table 4.** Summary of the Results from Dynamic Mechanical Analysis and Cross-Link Density Calculation from the Step Cured under Air of the Main Chain Polybenzoxazines

	poly (ALF8-BF)	poly (ALH12-BA)	poly (ARF12-BF)	poly (ARH12-BA)
molecular weight (g/g mol)	661	409	885	562
density (g/cm <sup>3</sup> )	1.54	1.13	1.52	1.15
$T_g$ (°C)	180	227	164	160
$T_g + 50$ (K)	503	550	487	483
storage modulus at $T_g + 50$ (MPa)	17.7		16.1	19.6
cross-link density (g mol/cm <sup>3</sup> )	4.23E-03		3.95E-03	4.88E-03
$M_c$	363.87		384.67	235.62
cross-link per unit	1.81		2.30	2.38

influenced by the hydrogen bonding in polybenzoxazine. However, the number of cross-links per chemical repeat unit is measured at 50 °C above the  $T_g$  (rubbery plateau modulus at  $T_g + 50$  °C). Therefore, the number of cross-links per chemical repeat unit is less influenced by the hydrogen bonding than the  $T_g$ . The intuitive discrepancy comes from this difference.

**3.2.5. Effect of the Atmosphere on Polymerization.** In order to study the effect of the atmosphere on the polymerization, the samples were step cured under nitrogen and the  $T_g$  of each material was determined by DMA analysis. The results of  $E'$

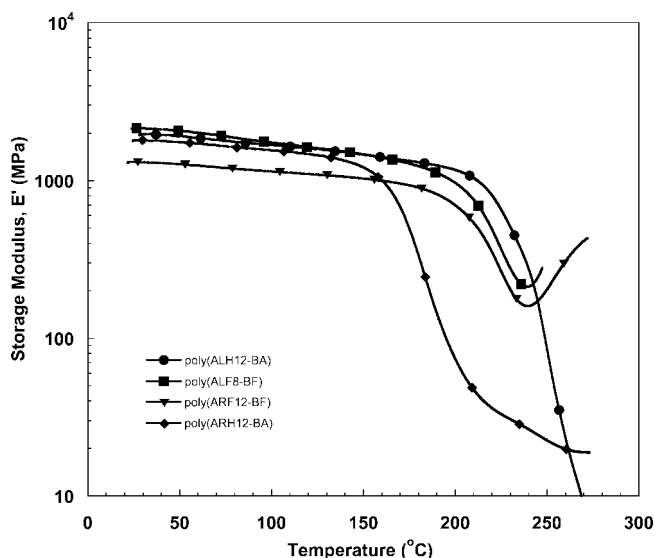


**Figure 14.** Storage moduli for the diamine-based series of polybenzoxazines step cured under nitrogen.

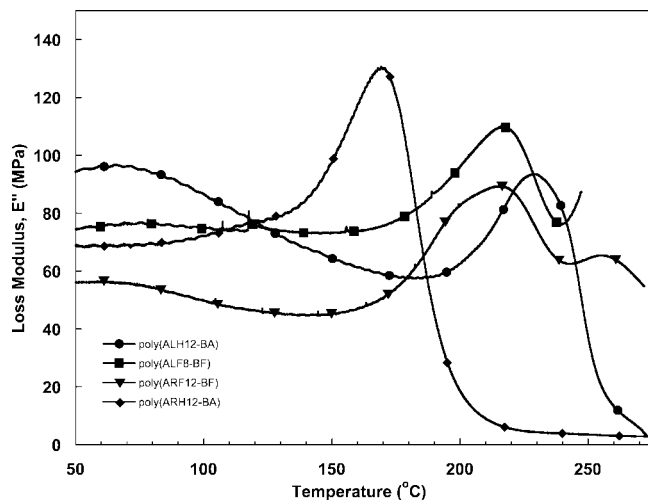


**Figure 15.** Loss moduli for the diamine-based series of polybenzoxazines step cured under nitrogen.

**Table 5. Summary of the Results from Dynamic Mechanical Analysis and Cross-Link Density Calculation from the Step Cured under Nitrogen of the Main Chain Polybenzoxazines**

	poly (ALF8-BF)	poly (ALH12-BA)	poly (ARF12-BF)	poly (ARH12-BA)
$T_g$ (°C)	216	250	211	173
$T_g + 50$ (K)	539	573	534	496
storage modulus at $T_g + 50$				23.2
cross-link density (g mol/cm <sup>3</sup> )				5.63E-03
$M_c$				204.3
cross-link per unit				2.75

and  $E''$  presented in Figures 14 and 15, respectively, show that the atmosphere affects the polymer structure, as the  $T_g$  of the materials increases by more than 40 °C for the fluorinated aromatic diamine-based compound and close to 35 °C for the fluorinated aliphatic diamine-based benzoxazine when polymerized under nitrogen. The hydrogenated diamine-based polybenzoxazines also show an increase by 23 and 13 °C, for **poly(ALH12-BA)** and **poly(ARH12-BA)**, respectively. A similar effect was observed for P-ad6; its glass transition temperature increased by more than 40 °C when polymerized under nitrogen.<sup>19</sup> These values for the modulus in the rubbery plateau were used to estimate the cross-link density and molecular weight between cross-links for the latter three polybenzoxazines and are summarized in Table 5. An explanation is readily apparent after infrared spectroscopic analysis of the polymers cured in each atmosphere presented in Figure 16 for **poly(ARF12-BF)**. Upon comparison of the fingerprint regions of each sample, it is obvious that an incomplete polymerization occurs when the polymer is cured under nitrogen as indicated by the absorbance at 940 cm<sup>-1</sup> and the corresponding band at 1510 cm<sup>-1</sup>. A carbonyl band at 1645 cm<sup>-1</sup>, which is consistent with the formation of substituted benzoquinone (SB), appears only for the material cured in the air environment. This has been identified previously as a product formed by the degradation of bisphenol-based polybenzoxazines.<sup>21</sup> The formation of the SB during the polymerization of the diamine-based polymers could have two detrimental effects on the network structure. First, it is well-known that the oxidation reaction occurs in the isopropylidene linkage and cleavage occurs to form an SB, with the reduction on the degree of cross-linking. Second, an SB would interfere with the hydrogen bonding as it turns the hydroxyl group into a carbonyl group that cannot participate in these interactions. Both would expect to adversely affect the glass transition temperature as well as mechanical properties

**Table 6. Percent of Water Absorption at Room Temperature of Step Cured Polybenzoxazines**

environment	time	poly (ALF8-BF)	poly (ARF12-BF)	poly (ALH12-BA)	poly (ARH12-BA)
in air	1 day	<0.1	<0.1	<0.1	<0.1
	1 week	<0.1	<0.1	0.4	0.6
in water	1 day	<0.1	<0.1	<0.1	0.8
	1 week	0.2	0.2	0.6	1.2

of step cured diamine-based polybenzoxazines. The degradation of the aromatic amine is shown by the decrease in the intensity of the absorbance band at 1615 cm<sup>-1</sup>.

**3.2.6. Water Absorption.** Since water possesses large dielectric constant value (78.5 at 25 °C), water absorption is required to be below 1% for an application where dielectric constant is of interest. Therefore, the hydrophobic character is required in low dielectric constant materials. The main chain polybenzoxazines synthesized have low water absorption; their values are listed in Table 6. The relative humidity of the air environment used was 100%. Both water saturated air and liquid water environments were at room temperature. Due to the highly limited sample quantities, we could not follow the ASTM procedure for water immersion test. The sample size used was 50 mm × 20 mm × 0.35 mm (average thickness). Therefore, the values reported in this paper should be considered only internally consistent and should not be compared with published results using ASTM standard. The thin sample thickness allowed the water uptake to reach near equilibrium rather quickly. Although the much longer immersion time is necessary to verify accurate water uptake value, it is believed that the reported value here is very close to the final value. The percent of water absorption are all below 1% except for **poly(ARH12-BA)**, which has a value of 1.2%. The results indicate that the fluorinated polybenzoxazines possess an outstanding property to resist water uptake.

**3.2.7. Dielectric Constant.** The dielectric constant ( $\epsilon$ ) is directly related to the polarizability of the material. Therefore, it is strongly dependent on its chemical structure.<sup>33</sup> Table 7 presents the dielectric constant value and the dissipation factor,  $\tan \delta$ , for all the compounds. Due to the limited quantity of compound synthesized, accurate values must await for further detailed study in the future. A value of 2.2 was observed for **poly(ALF8-BF)**, this is the lowest for all the compounds. This value is lower than 2.4 obtained for **poly(ARF12-BF)** because saturated hydrocarbons are significantly less polarizable than the species which are unsaturated, conjugated, or with polarizable phenyl groups.

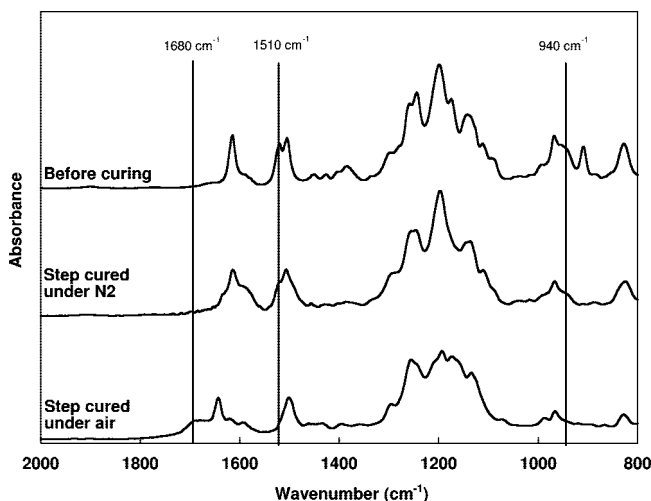


**Figure 16.** Infrared spectroscopy for the fingerprint region of ARF12-BF and poly(ARF12-BF) under inert atmosphere and under air at 10<sup>9</sup> Hz and 25 °C.



**Table 7. Dielectric Constant and Dissipation Factor of the Diamine-Based Polybenzoxazines at 10<sup>9</sup> Hz and 25 °C**

compound	dielectric constant	dissipation factor (tan $\delta$ )
poly(ALF8-BF)	2.2	0.008
poly(ALH12-BA)	3.0	0.010
poly(ARF12-BF)	2.4	0.024
poly(ARH12-BA)	2.9	0.010
poly(ALF8-BA)	2.6	0.014
poly(ARF12-BF) <sup>a</sup> (1)	2.4	---
poly(ARF12-BF) <sup>a</sup> (2)	2.3	---

<sup>a</sup> Dielectric constant was obtained with the refractive index at 10<sup>14</sup>Hz and 25 °C of the diamine-based benzoxazines step cured (1) under air and (2) under nitrogen.

In general, the value of  $\epsilon$  can be lowered by breaking off the conjugated system or decreasing the number of phenyl group in the monomer. However, these alterations compromise the thermal stability, as shown by the TGA thermograms of the samples. The substitution of the methylene group for a benzyl group increases the onset degradation by 20 °C and the 5% weight loss temperature ( $T_{d5}$ ) by more than 50 °C. Substitution of H with F and  $-\text{CH}_3$  with  $-\text{CF}_3$  group decreases the electronic polarizability due to strong electron-withdrawing inductive effect of the fluorine atom. This effect is clear when the value for the aromatic diamine-based polymers are compared; the substitution decreases the dielectric constant from 2.9 to 2.4. It is important to mention that the thermal stability as well as  $T_g$  are increased by the substitution. The substitution of bisphenol A with bisphenol AF shows a decrease in the dielectric constant by 0.34 because the bulky  $-\text{CF}_3$  group is able to reduce efficient molecular packing and increase the free volume.

To analyze the effect of the curing conditions, ARF12-BF was cured under air and nitrogen. This compound was selected because it showed the highest increases in  $T_g$  when cured under nitrogen. The dielectric constant was obtained from the refractive index; The values obtained varies by less than 1% suggesting that the curing conditions does not significantly affect the value obtained.

#### 4. Conclusions

Two aromatic and two aliphatic diamine-based polybenzoxazine with the oxazine ring in the main chain have been successfully synthesized. The structures of these polybenzoxazines have been verified by NMR and FTIR. The thermal stability of the step-cured polymer was determined by the nature of the group next to the amine. The  $T_g$  of the materials was strongly influenced by the curing conditions. The fluorination reduces the dielectric constant and improves the thermal stability.

**Acknowledgment.** The authors are grateful for the financial support of Sekisui Integrated Research.

**Supporting Information Available.** <sup>19</sup>F NMR and FTIR spectra. This material is available free of charge via the Internet at <http://pubs.acs.org>

#### References and Notes

- (1) (a) Liu, J.; Ishida, H. *Polym. Polym. Comp.* **2002**, *10*, 191–203. (b) Kanchanasopa, M.; Nantaya, Y.; Hemvichian, K.; Ishida, H. *Polym. Polym. Comp.* **2001**, *9*, 367–375.
- (2) Agag, T.; Takeichi, T. *Macromolecules* **2001**, *34*, 7257–7263.
- (3) Brunovska, Z.; Lyon, R.; Ishida, H. *Thermo Acta* **2000**, *35*, 7–358, 195–203.
- (4) Sander, D. P.; Ishida, H. *J. Polym. Sci. Part B, Polym. Phys.* **2000**, *38*, 3289–3301.
- (5) Kim, H. D.; Brunovska, Z.; Ishida, H. *Polymer* **1999**, *40*, 6565–6573.
- (6) Ishida, H.; Allen, D. J. *J. Polym. Sci., Part B: Polym. Phys.* **1996**, *34*, 1019–1030.
- (7) Brunovska, Z.; Liu, J. *Macromol. Chem. Phys.* **1999**, *200*, 1745–1752.
- (8) Ning, X.; Ishida, H. *J. Polym. Sci., Part A: Polym. Chem.* **1994**, *32*, 1121–1129.
- (9) Riess, G.; Schwob, J. M.; Guth, G.; Roche, M.; Laude, B. In *Advances in Polymer Synthesis*, *Polymer Science & Technology*; Culbertson B. M., McGrath, J. E., Eds.; Plenum: New York, 1985; Vol. 31, p 27.
- (10) Wang, Y. X.; Ishida, H. *J. Appl. Polym. Sci.* **2002**, *86*, 2953–2966.
- (11) Laobuthee, A.; Chirachanchai, S.; Ishida, H.; Tashiro, K. *J. Am. Chem. Soc.* **2001**, *123*, 9947–9955.
- (12) Allen, D. J.; Ishida, H. *J. Appl. Polym. Sci.* **2006**, *101*, 2798–2809.
- (13) (a) Liu, J. P. *Ph.D. Thesis*, Case Western Reserve University, Cleveland, Ohio, 1994; pp176–214. (b) Liu J. P.; Ishida, H. In *The Polymeric Materials Encyclopedia*; Salamone, J. C., Ed.; CRC Press: Boca Raton, FL, 1996; pp 484–494.
- (14) (a) Chernykh, A.; Liu, J.; Ishida, H. *Polymer* **2006**, *47*, 7664–7669. (b) Agag, T.; Takeichi, T. *J. Polym. Sci. A: Polym. Chem.* **2007**, *45*, 1878–1888. (c) B. Kiskan, B.; Yagci, Y.; Ishida, H. *J. Polym. Sci.: Part A: Polym. Chem.* **2008**, *46*, 414–420. (d) Nagai, A.; Kamei, Y.; Wang, X. S.; Omura, M.; Sudo, A.; Nishida, H.; Kawamoto, E.; Endo, T. *J. Polym. Sci., Part A: Polym. Chem.* **2008**, *46*, 2316–2325. (e) (a review Ghosh, N. N.; Kiskan, B.; Yagci, Y. *Prog. Polym. Sci.* **2007**, *32*, 1344–1391.
- (15) Su, Y.-C.; Chang, F.-C. *Polymer* **2003**, *44*, 7989–7996.
- (16) Su, Y.-C.; Chen, W.-C.; Ou, K.-L.; Chang, F. C. *Polymer* **2005**, *46*, 3758–3766.
- (17) Snow, A. W.; Buckley, L. J. In *Fluoropolymers I: Synthesis*; Hougham, et al., Eds.; Plenum Press: New York, 1999.
- (18) Velez-Herrera, P.; Ishida, H. Submitted for publication.
- (19) Van Alphen, J. *Recl. Trav. Chim.* **1940**, *59*, 580.
- (20) Green, F. D.; Edwards, B. E. *J. Org. Chem.* **1958**, *23*, 487.
- (21) Macko, J. A.; Ishida, H. *J. Polym. Sci., Part B: Polym. Phys.* **2000**, *38*, 2682–2701.
- (22) Hemvichian, K.; Laobuthee, A.; Chirachanchai, S.; Ishida, H. *Polym. Degrad. Stab.* **2002**, *76*, 1–15.
- (23) Hemvichian, K.; Kim, H. D.; Ishida, H. *Polym. Degrad. Stab.* **2005**, *87*, 213–224.
- (24) Kim, H. D.; Ishida, H. *Macromol. Symp.* **2003**, *195*, 123–140.
- (25) Kim, H. D.; Ishida, H. *J. Phys. Chem. A* **2002**, *106*, 3271–3280.
- (26) Dunkers, J.; Ishida, H. *Spectrochim. Acta* **1995**, *51A*, 855–867.
- (27) Colthup, N. B.; Daly, L. H.; Wiberley, S. E. *Introduction to Infrared and Raman Spectroscopy*; Academic Press: New York, 1990.
- (28) Espinosa, M. A.; Cadiz, V.; Galia, M. *J. Appl. Polym. Sci.* **2003**, *90*, 470–481.
- (29) Odian G. *Principles of Polymerization*; Wiley: New York, 1991.
- (30) Dunkers, J.; Zarate, E. A.; Ishida, H. *J. Phys. Chem.* **1996**, *100*, 13514–13520.
- (31) Ishida, H.; Sanders, D. P. *Macromolecules* **2000**, *33*, 8149–8157.
- (32) Ferry, J. D. *Viscoelastic Properties of Polymers*; Wiley: New York, 1980.
- (33) Hougham, G.; Tesoro, G.; Viehbeck, A.; Chapple-Soko, J. D. *Macromolecules* **1994**, *27*, 5964–5971.

MA801253A